Robust flight-to-gate assignment with landside capacity constraints

L'Ortye, J.; Mitici, M.; Visser, H. G.

DOI
10.1080/03081060.2021.1919347

Publication date
2021

Document Version
Final published version

Published in
Transportation Planning and Technology

Routledge
Taylor & Francis Group

Transportation Planning and Technology

ISSN: (Print) (Online) Journal homepage: https://www.tandfonline.com/loi/gtpt20

Robust flight-to-gate assignment with landside capacity constraints

J. L'Ortye, M. Mitici & H.G. Visser

To cite this article: J. L'Ortye, M. Mitici & H.G. Visser (2021) Robust flight-to-gate assignment with landside capacity constraints, Transportation Planning and Technology, 44:4, 356-377, DOI: 10.1080/03081060.2021.1919347

To link to this article: https://doi.org/10.1080/03081060.2021.1919347

Published online: 27 Apr 2021.

TRANSPORTATION PLANNING AND TECHNOLOGY
2021, VOL. 44, NO. 4, 356–377
https://doi.org/10.1080/03081060.2021.1919347

Routledge
Taylor & Francis Group

Robust flight-to-gate assignment with landside capacity constraints

J. L'Ortye, M. Mitici and H.G. Visser

Faculty of Aerospace Engineering, Delft University of Technology, Delft, The Netherlands

ABSTRACT

At the interface between airport airside and landside operations, the assignment of flights to gates is key to ensure efficient operations and a high quality of service for passengers. We propose a mixed-integer linear program for an integrated flight-to-gate assignment that considers both airside as well as landside constraints on the capabilities of facilities such as check-in, security or transfer to handle passengers. Moreover, our assignment is robust in that it constrains the probability of multiple flights being assigned to the same gate. Having obtained an integrated, robust flight-to-gate assignment, we analyse the associated quality of service at the landside facilities. Overall, our model supports the design of a robust, integrated airside-landside assignment of flights to gates at an airport.

ARTICLE HISTORY
Received 16 April 2020
Accepted 8 January 2021

KEYWORDS
Flight-to-gate; landside airport constraints; robust optimization; flight splitting; Amsterdam Airport Schiphol

1. Introduction

At large airports, the process of assigning flights to gates is complex, involving the allocation of limited airside resources (e.g. gates), as well as meeting quality of service requirements for the passengers inside the terminals. This becomes even more involved when considering the uncertainty in the arrival and departure flight times.

In recent years, several mathematical formulations have been proposed to solve the flight-to-gate assignment problem (FGAP) (Bouras et al. 2014). However, these approaches consider only airside constraints and, in some cases, passenger-specific requirements, such as minimal passenger walking distance to the gates. However, the impact of the flight-to-gate assignment on the ability of the landside facilities (checkin, security, transfer facilities) to provide a sufficient level of service inside the terminal, e.g. waiting time at these facilities, has not been considered. For instance, a gate assignment can be such that all airside constraints are satisfied and the total passenger walking distance is minimized. However, following this assignment, the flow of passengers at a landside facility may mean that the number of passengers waiting at this facility increases significantly. To address this, in this paper we determine flight-to-gate assignments such that the maximum number of passengers or the maximum passenger waiting time is limited at all landside facilities.

CONTACT M. Mitici m.a.mitici@tudelft.nl Faculty of Aerospace Engineering, Delft University of Technology, HS 2926 Delft, The Netherlands

Equally important, several robust FGAP models have been proposed in recent years. In Mangoubi and Mathaisel (1985), Yan and Chang (1997) and Yan and Huo (2001), the authors propose FGAP models which implement fixed buffer times as a means to manage deviations from flight schedules. In Bolat (2000) and Diepen et al. (2012), the authors maximize gate idle time, i.e. the time a gate is not used. In Castaing et al. (2016) and Yu, Zhang, and Lau (2017), the FGAP models aim to minimize the duration and number of gate conflicts, respectively. In Kim et al. (2017) and Seker and Noyan (2012) FGAP models are developed that aim at minimizing gate conflicts. Also, Schaijk and Visser (2017) consider stochastic arrival/departure times, while aiming at minimizing the flight overlap probability, i.e. the probability that more flights are assigned to the same gate at the same time. Most of these models, however, consider only airside-related constraints and objectives. In some cases, the models are also passenger-centric such as Kim et al. (2017), Mangoubi and Mathaisel (1985), Yan and Huo (2001) and Yu, Zhang, and Lau (2016) where the aim is to minimize passenger walking distance or transit time. To complement this work, we propose a robust and integrated airside-landside FGAP model that includes constraints for both the airside and the landside facilities.

For the analysis of the landside of an airport, Manataki and Zografos (2009) describe a high-level architecture of a large airport. The authors consider an airport consisting of an unrestricted area, a controlled area, gates and arrival-controlled airport functional areas. Li et al. (2018) model the airport security facilities as networks of queues. Kusumaningtyas and Lodewijks (2013) provide a detailed diagram of main terminal facilities and the flows of passengers, while van Dijk and van der Sluis (2006) characterize the flows of passengers arriving at a large airport by means of a triangular shaped distribution. Following up on these approaches, we propose a generic layout for an airport terminal, we identify the main landside facilities within a terminal and characterize the passenger streams that use these facilities. These models are used as input for our robust, integrated airside-landside FGAP model.

In this paper we propose a robust model that considers several strategies to manage landside and airside constraints. Here, by landside constraints we mean that: i) the number of passengers (demand) at any landside facility is constrained by a maximum capacity or ii) the maximum passenger waiting time at these facilities is limited. In doing so, we consider the possibility to split a flight into multiple segments, where each segment is allocated to different gates or parking areas. This model extends the robust FGAP model by Schaijk and Visser (2017), which considers airside constraints only and no options for flight splitting. In this paper we propose three airside-landside operational strategies: i) where only airside constraints are active (baseline), ii) where both airside and landside constraints are active, and passenger demand cannot exceed a fixed capacity at the landside facilities and iii) where both airside and landside constraints are active, and the maximum passenger waiting time at a facility is limited. Overall, our approach provides support for the management of both airside and landside operations, in an integrated manner. We illustrate our approach with a case study of Amsterdam Airport Schiphol (AMS).

2. Flight-to-gate assignment with airside and landside constraints

In this section we introduce a robust flight-to-gate assignment model with airside and landside constraints. Here, we assume a discrete-time model. First, we discuss the option of splitting a flight into segments. Next, we describe the notion of presence

probabilities of flight segments, which is used to achieve model robustness. Further, we introduce a passenger demand model within a facility in an airport terminal. Lastly, we formulate the robust, landside-airside flight-to-gate assignment model.

2.1. The option of splitting a flight into segments

We assume that a flight has a scheduled arrival time (STA) and a scheduled departure time (STD) at an airport. We define the presence time of a flight to be equal to the time between the STA and STD of that flight. During this time, a flight can be split into flight segments. We consider three possible types of flight segments corresponding to:

i) passengers disembarking and/or boarding an aircraft, ii) the aircraft being towed and, iii) the aircraft being parked. We define a functional flight segment as a flight segment where passengers disembark and/or board an aircraft. We consider a planning horizon of operations between 00:00 and 23:59 on the same calendar day. Below we characterize: 1) flights without an overnight-stay, 2) flights with an overnight-stay and a morning departure and 3) flights with an evening arrival and an overnight-stay.

1. Flights without overnight-stay – splitting options

The STA and STD of flights without an overnight-stay are both within the planning horizon. We define three different flight splitting options for such a flight, which include: 1) the flight is not split and is assigned to the one gate from its STA until its STD (see segment 1 in Figure 1); 2) the flight is split into three segments, including a functional flight segment, a towing segment and a second functional flight segment (see segments 2,3,4 in Figure 1); and 3) the flight is split into five segments, including a functional flight segment, a towing segment, a parking segment, a second towing segment and a second functional flight segment (see segments 5,6,7,8,9 in Figure 1).

2. Flights with morning departure – splitting options

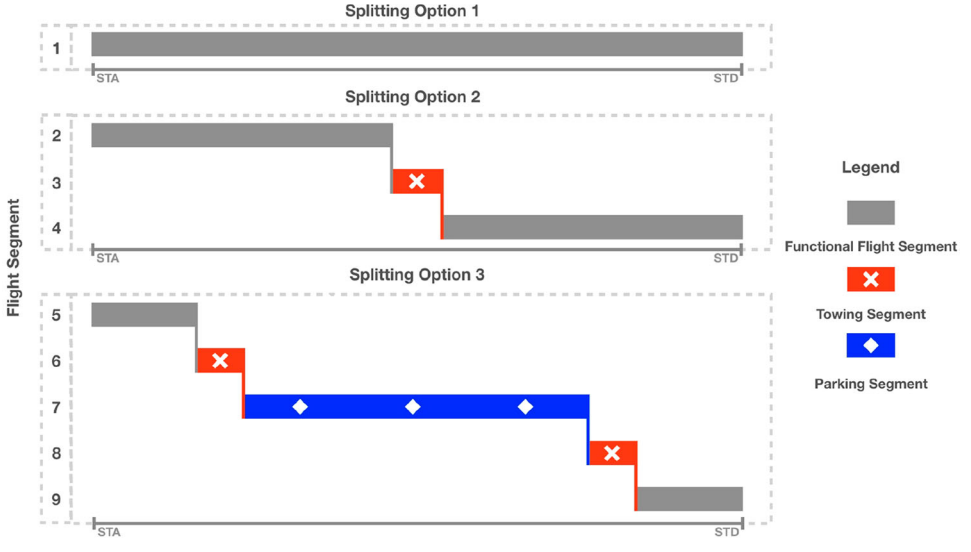

Figure 1. Example of three splitting options for flights without overnight-stay.

The STA of a flight with a morning departure is outside of the planning horizon. Flight splitting options for a flight with a morning departure include: 4) the flight is not split and is assigned to one gate from 00:00 until its STD (see segment 1 in Figure 2); and 5) the flight is split into three segments: a parking, a towing and a functional segment where passengers board the aircraft (see segments 2,3,4 in Figure 2).

3. Flights with evening arrival – splitting options

The STD of a flight with an evening arrival is outside the planning horizon. Flight splitting options for such flights include: 6) the flight is not split and is assigned to one gate from its STA until 23:59 (see segment 1 in Figure 3); and 7) the flight is split into three segments: a functional segment where passengers disembark, a towing and a parking segment (see segments 2,3,4 in Figure 3).

2.2. Presence probability of flight segments

In this section we introduce the presence probability of flight segments, i.e. the probability that a flight segment is present at the airport at a particular time. Let F denote the set of all arriving and departing flights at the airport in a day, where N denotes the set of all possible flight segments created by applying the flight splitting options outlined above, M denotes the set of gates at the airport, and $S_{l,t} \subseteq N$ is the set that contains all possible flight segments of flight l at time step t. We consider the planning horizon to be discretised in time steps of 5 min, with a total of K time steps for the entire planning horizon of 1 d of operations.

We define $p_{i,l,t}$ as the presence probability of flight segment$i \in S_{l,t}$ at time step $t \in K$, which is derived from the presence probability of flight $l \in F$:

$$p_{i,l,t} = fp_{l,t}, \quad i \in S_{l,t}, \quad t \in K \tag{1}$$

where $fp_{l,t}$ is the presence probability of flight l from which flight segment i is derived.

We determine the flight presence probability for a flight as follows (Schaijk and Visser 2017):

$$fp_{l,t} = \max\{fp_{l,t,\,arr} - |1 - fp_{l,t,\,dep}|, 0\}, \; l \in F, \; t \in K, \tag{2}$$

where $fp_{l,t}$ denotes the flight presence of flight l at time step t, $fp_{l,t,\,arr}$ is the arrival flight

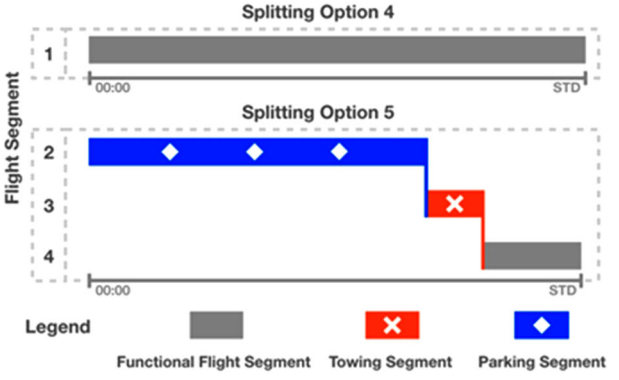

Figure 2. Flights with overnight-stay and morning departure.

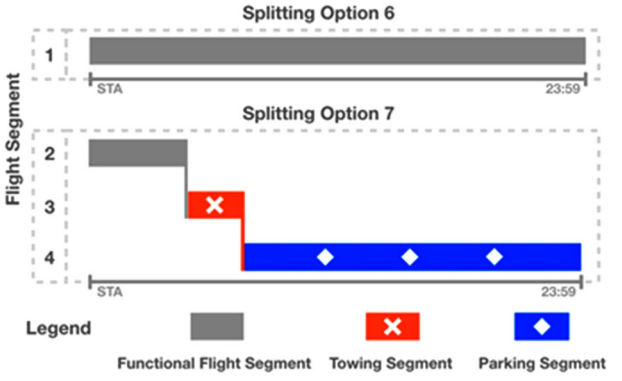

Figure 3. Flights with evening arrival and overnight-stay.

presence probability of flight l at time step t and $fp_{l,t,\,dep}$ is the departure flight presence probability of flight l at time step t. Figure 4 gives an example of $fp_{l,t,\,arr}$, $fp_{l,t,dep}$ and $fp_{l,t}$ for a flight l.

2.3. Passenger demand model for landside facilities

We defineN_a and N_d to be the set of flight segments where passengers disembark and board aircraft, respectively, $N_a \cup N_d \subseteq N$. We define H as the set of facilities. Let T denote the set of terminals at the airport. Let $D_{i,p,q,t}$ denote the number of passengers of flight segment $i \in N_a \cup N_d$ that use facility $p \in H$ in terminal $q \in T$ during time step t. Then $D_{i,p,q,t}$ is computed as follows:

$$D_{i,\,p,\,q,\,t} \;=\; \rho_{i,p} \cdot \gamma_{i,p,q,t}\,,\; i \in N_a \cup_d^N,\; p \in H,\; q \in T,\; t \in K, \tag{3}$$

where $\rho_{i,p}$ is the total number of passengers from flight segment i that use facility p and $\gamma_{i,p,q,t}$ denotes the fraction of the total number of passengers from flight segment i that use facility p in terminal q during time step t.

First, we assume that $\rho_{i,p} = \eta_i \cdot c$, where η_i denotes the estimated number of seats on the aircraft serving flight segment i and c is a constant.

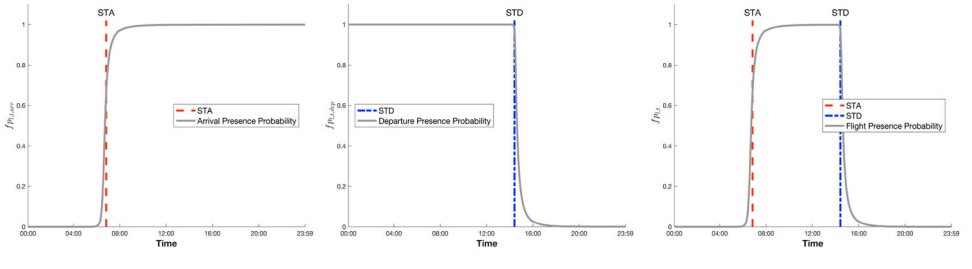

a. $fp_{l,t,arr}$ b. $fp_{l,t,d}$ c. $fp_{l,t}$

Figure 4. Example of $p_{l,t,\,arr}$, $fp_{l,t,dep}$ and $fp_{l,t}$ for a flight l without an overnight-stay. This flight has a STA = 06:50 and STD = 14:25.

Second, we assume that the distribution of the fraction of passengers from flight segment i using facility p in terminal q during time step t follows an elliptical distribution (Chun and Mak 1999). The height of the elliptical distribution is given by $\gamma_{i,p,q,t}$. The support of this distribution is $[t^e_{i,p,q} - t^s_{i,p,q}]$, where $t^s_{i,p,q}$ and $t^e_{i,p,q}$ denote the start and end time for passengers arriving/departing with flight segment i to pass through facility p in terminal q.

An example of values of $\lambda_{i,\,p,\,q,\,t}$ and $\gamma_{i,p,q,t}$ are given in Figures 5 and 6 for facility (1) and Figures 7 and 8 for facility (2) in terminal q over t ∈ [115,155], respectively. By construction, $\max_t \lambda_{i,\,p,\,q,\,t} = 1$ and $\sum_{t \in K} \gamma_{i,p,q,t} = 1$ for $i \in N_a \cup N_d$, $p \in H$,$q \in T$ and, therefore, all arriving/departing passengers on flight i are accounted for.

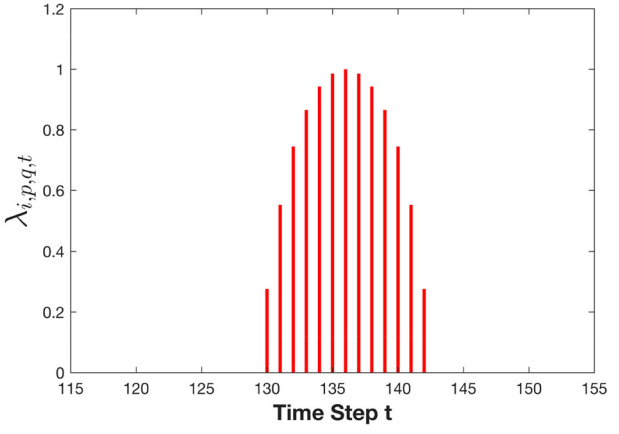

Figure 5. Example value of $\lambda_{i,\,p,\,q,\,t}$ of flight segment i at facility (1) in terminal q during time step t, with $t^s_{i,p,q}$= 130, $t^e_{i,p,q}$= 142, $\lambda_{i,\,p,\,q,\,t} \leq 1$.

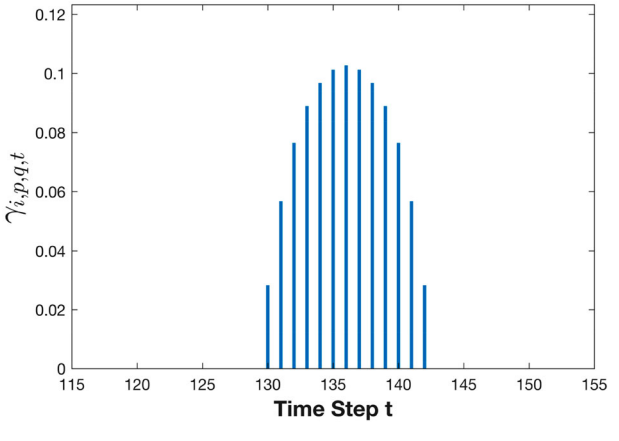

Figure 6. Example value of $\gamma_{i,p,q,t}$ of flight segment i at facility (1) in terminal q during time step t, with $t^s_{i,p,q}$= 130, $t^e_{i,p,q}$= 142, $\sum_t \gamma_{i,p,q,t} = 1$.

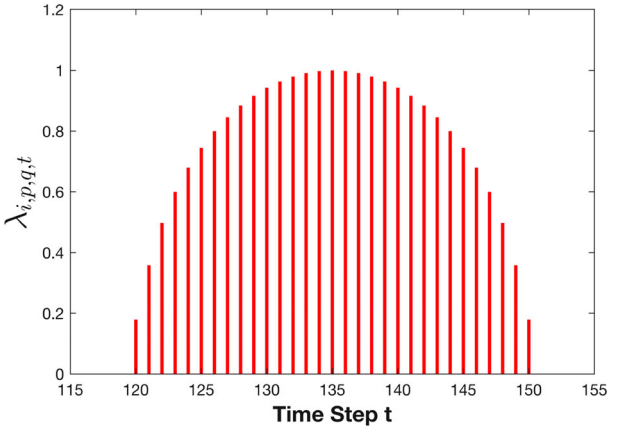

Figure 7. Example value of $\lambda_{i,\,p,\,q,\,t}$ of flight segment i at facility (2) in terminal q during time step t, with $t^s_{i,p,q}$= 120, $t^e_{i,p,q}$= 150, $\sum_t \lambda_{i,p,q,t} \leq 1$.

2.4. Mathematical model – robust flight-to-gate assignment with airside and landside constraints

In this section we describe the decision variables, objective function and constraints of the robust flight-to-gate assignment model with airside and landside constraints.

Decision variables

We assume that a flight segment $i \in N$ can be assigned only to a subset $G_i^1 \subseteq M$ of gates. We consider the decision variables in equation (4) – (6):

$$x_{i,j,t} = \begin{cases} 1, & \text{if flight segment } i \text{ is assigned to gate } j \text{ at time } t \\ 0, & \text{otherwise} \end{cases}, \quad i \in N,\ j \in G_i^1,\ t \in K. \tag{4}$$

$$z_{i,j,q} = \begin{cases} 1, & \text{if flight segment } i \text{ is assigned to gate } j \text{ and its departing passenger flow is assigned to terminal } q \\ 0, & \text{otherwise} \end{cases}, \quad i \in N_d,\ j \in G_i^1,\ q \in T, \tag{5}$$

$$y_{p,q,t} = \sum_{i \in N_a \cup_d^N} \sum_{j \in G_i^1} D_{i,p,q,t}\, z_{i,j,q},\ p \in H,\ q \in T,\ t \in K, \tag{6}$$

where $y_{p,q,t}$ denotes the number of passengers that use facility p in terminal q during time step t.

Objective function

We consider the following objective function:

$$\min_{\mathrm{x_{i,j,t,j,t}}\,,\,\mathrm{z_{i,j,t}}} \quad Z = \sum_{i \in N} \sum_{j \in G_i^1} \sum_{t \in K} c^a_{i,j} x_{i,j,t} + w_{al} \sum_{i \in N_a \cup_d^N} \sum_{j \in G_j^1} \sum_{q \in T} c^l_{i,j,q}\, z_{i,j,q}, \tag{7}$$

where $c^a_{i,j}$ and $c^l_{i,j,q}$ are time-invariant airside and landside cost coefficients, respectively, and w_{al} scales the cost of the landside element accordingly.

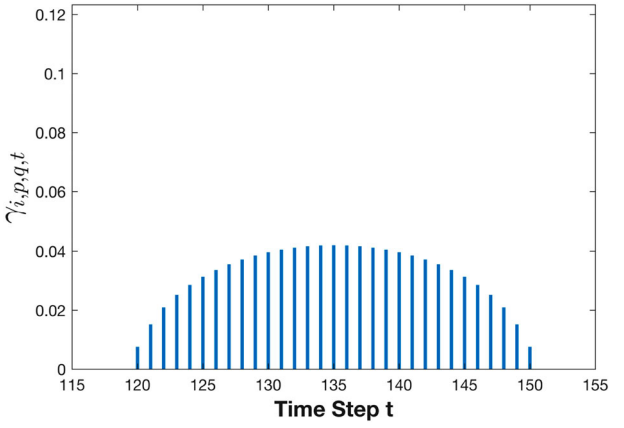

Figure 8. Example value of $\gamma_{i,p,q,t}$ of flight segment i at facility (2) in terminal q during time step t, with $t^s_{i,p,q}$= 120, $t^e_{i,p,q}$= 150, $\sum_t \gamma_{i,p,q,t} = 1$.

The objective function consists of two elements. The first element $\sum_{i\in N}\sum_{j\in G_i^1}\sum_{t\in K} c^a_{i,j}x_{i,j,t}$ expresses the cost of assigning flight segment $i \in N$, to gate $j \in G_i^1$ at time $t \in K$. The second element $\sum_{i\in N_a\cup N_d}\sum_{j\in G_j^1}\sum_{q\in T} c^l_{i,j,q}\, z_{i,j,q}$ expresses the cost of assigning flight segment $i \in N_a \cup N_d$ to gate $j \in G_i^1$ and its departing passenger stream to terminal $q \in T$.

The value of $c^a_{i,j}$ is based on size, customs and type requirements of flight $i \in N$ and gate $j \in G_i^1$, as follows:

$$c^a_{i,j} = c^{Customs}_{i,j} + c^{Size}_{i,j} + c^{Type}_{i,j}. \tag{8}$$

where i) $c^{Customs}_{i,j}$is a customs cost of assigning flight segment i to gate j, ii) $c^{Size}_{i,j}$ is the size cost of assigning flight segment i to gate j of a given size and iii) $c^{Type}_{i,j}$ denotes the aircraft-gate type cost which is a function of the type of flight segment i and the type of gate j (Schaijk and Visser 2017). To determine w_{al} we solve:

$$\sum_{i\in N}\sum_{j\in G_i^1} c^a_{i,j}\,\frac{1}{\sum_{i\in N}|G_i^1|} = w_{al}\sum_{i\in N}\sum_{j\in G_i^1} c^l_{i,j,q}\,\frac{1}{|T|\sum_{i\in N}|G_i^1|}. \tag{9}$$

As an example, we consider $N = \{1, 2\}$, $M = \{1, 2, 3\}$ and $T = \{1, 2\}$ with $G_1^1 = \{1\}$ and $G_2^1 = \{1, 2, 3\}$, and departing passenger flows of gates $j \in M$ can be assigned to terminals $q \in T$. The left side of equation (9) becomes $c_{1,1}\cdot\frac{1}{4} + c_{2,1}\cdot\frac{1}{4} + c_{2,2}\cdot\frac{1}{4} + c_{2,3}\cdot\frac{1}{4}$ and the right-hand side becomes $c_{1,1,1}\cdot\frac{1}{8} + c_{1,1,2}\cdot\frac{1}{8} + \ldots + c_{2,3,2}\cdot\frac{1}{8}$. The value of w_{al} is set such that equation (9) holds.

Constraints

Prior to discussing the constraints, we introduce the following notation:

$$s_{i,l,t} = \begin{cases} 1, & \textit{if flight segment } i \in S_{l,t} \textit{ belonging to flight } l \\ & \textit{has a non} - \textit{zero probability to be present at time } t, \\ 0, & \textit{otherwise}. \end{cases} \tag{10}$$

As an example, we consider Figure 9, for a given flight l. We assume that the flight splitting options 1–3 can be applied to flight l. Then, $s_{1,l,t} = 1$ for $STA \leq t \leq STD$, $s_{2,l,t} = 1$ for $STA \leq t \leq h_3$, $s_{3,l,t} = 1$ for $h_3 < t \leq h_4$, $s_{4,l,t} = 1$ for $h_4 < t \leq STD$, $s_{5,l,t} = 1$ for $STA \leq t \leq h1$, $s_{6,l,t} = 1$ for $h1 < t \leq h2$, $s_{7,l,t} = 1$ for $h2 < t \leq h5$, $s_{8,l,t} = 1$ for $h_5 < t \leq h_6$, $s_{8,l,t} = 1$ for $h_6 < t \leq STD$.

$$\sum_{l \in F} \sum_{i \in S_{l,t}} s_{i,l,t}\, x_{i,j,t} \leq 1, \quad \forall\, j \in M,\ \forall\, t \in K$$

$$s_{i,l,t}\, x_{i,j,t+1} - \ s_{i,l,t+1}\, x_{i,j,t} = 0,\ \forall l \in F,\ \forall i \in S_{l,t},\ \forall j$$

We now present the set of landside and airside constraints for our FGAP model:

$$\sum_{l \in F} \sum_{i \in S_{l,t}} s_{i,l,t}\, x_{i,j,t} \leq 1, \quad \forall\, j \in M,\ \forall\, t \in K \tag{11}$$

$$s_{i,l,t}\, x_{i,j,t+1} - \ s_{i,l,t+1}\, x_{i,j,t} = 0, \quad \forall l \in F,\ \forall i \in S_{l,t},\ \forall j \in G_i^1,\ \forall t \in K \tag{12}$$

$$\sum_{i \in S_{l,t}} \sum_{j \in G_i^1} s_{i,l,t}\, x_{i,j,t} = 1, \quad \forall l \in F, \forall t \in K \tag{13}$$

$$x_{i,j,t} = \sum_{q \in T} z_{i,j,q}, \quad \forall i \in N_a,\ \forall j \in G_i^1,\ t = STA_i \tag{14}$$

$$x_{i,j,t} = \sum_{q \in T} z_{i,j,q}, \quad \forall i \in N_a,\ \forall j \in G_i^1,\ \forall\, t = STD_i \tag{15}$$

$$y_{p,q,t} = \sum_{i \in N_a \cup_d^N} \sum_{j \in G_i^1} D_{i,p,q,t}\, z_{i,j,q},\ \forall\, p \in H,\ \forall\, q \in T,\ \forall t \in K \tag{16}$$

$$y_{p,q,t} \leq b_{p,q,t}, \quad \forall\, p \in H,\ \forall\, q \in T,\ \forall t \in K \tag{17}$$

Constraint (11) ensures that only one flight segment and only one is assigned to a gate in a given time step. Constraint (12) ensures that if a flight segment is assigned to a particular gate at a particular time, then this is not switched to a different gate in a subsequent time step (Schaijk and Visser 2017). Constraint (13) ensures that, for each time step, a flight has a non-zero probability of being present at the airport; exactly one segment for the flight is assigned to the gate. Together with constraint (12), this constraint ensures that one and only one of the flight splitting options is selected. Constraint (13) extends constraint (3) in Schaijk and Visser (2017) to allow for flight splitting by summing over the set of possible flight splitting options $S_{l,t}$. Constraints (14) and (15) indicate that for every flight segment $i \in N_a \cup N_d$ assigned to gate $j \in G_i^1$, departing passenger streams can only be directed to one terminal. If $x_{i,j,t}$ for $t \in \{STA_i,\ STD_i\}$ is equal

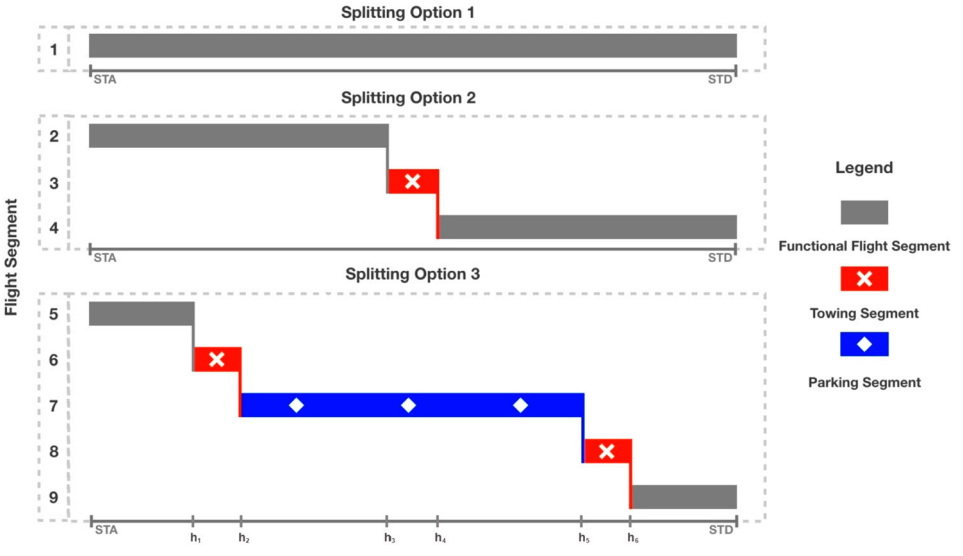

Figure 9. Example of 3 splitting options for flights without overnight-stay.

to 1, only one of the decision variables $z_{i,j,q}$ for $q \in T$ can take a value of 1. If $x_{i,j,t}$ for $t \in \{STA_i,\ STD_i\}$ is equal to 0, $z_{i,j,q}$ for $q \in T$ are automatically set to 0. Constraint (16) indicates that the passenger demand imposed on facility $p \in H$ in terminal $q \in T$ at time $T \in K$ is a function of the decision variables $z_{i,j,q}$. Constraint (17) sets an upper bound to the value of $y_{p,q,t}$ denoted by the parameter $b_{p,q,t}$.

Lastly, to have a robust FGAP model with landside and airside constraints, we replace constraint (11) to ensure that the overlap probability that two flight segments are assigned to the same gate (overlap probability) is below a user-specified threshold r, as follows (Schaijk and Visser 2017):

$$\sum_{l \in F} \sum_{i \in S_{l,t}} f(p_{i,l,t}, r) \cdot p_{i,l,t}\ x_{i,j,t} \leq 1, \qquad \forall j \in M,\ \forall t \in K \tag{18}$$

where we make use of a scaling function $f(p_{i,l,t}, r)$. We determine $f(p_{i,l,t}, r)$ as follows (Schaijk and Visser 2017). We define the maximum, user-defined, overlap probability r as:

$$r = p_{i,l,t} \cdot p_{max} \tag{19}$$

where p_{max} is the maximum probability of a different flight segment to be assigned to the same gate at the same time without exceeding the maximum overlap probability threshold r. We next define a scaling function $f(p_{i,l,t}, r)$ such that

$$f(p_{i,l,t}, r) \cdot\ p_{i,l,t} + f(p_{i,l,t}, r) \cdot\ p_{max} = 1. \tag{20}$$

Solving (19) and (20), we have (Schaijk and Visser 2017):

$$f(p_{i,l,t}, r) = \frac{p_{i,l,t}}{r + p_{i,l,t}^2}. \tag{21}$$

Now, replacing constraint (11) by (18), we obtain a robust assignment of flight segments.

3. Landside constraints – specifying $b_{p,q,t}$ in the passenger demand constraint (17) of our robust FGAP model

As landside constraints, we constrain passenger demand at the landside facilities by specifying; i) a maximum number of passengers allowed at a landside facility, i.e. a fixed declared capacity, or ii) limits for the maximum passenger waiting time at a landside facility. Formally, the value of the parameter $b_{p,q,t}$ in constraint (17) is set such that: i) only airside constraints are active (baseline model), ii) both airside and landside constraints are active, and passenger demand cannot exceed a declared landside capacity, and iii) both airside and landside constraintS are active, and the landside passenger constraints are driven by the expected maximum passenger waiting time. We discuss each of these three strategies below:

i) Active airside constraints and inactive landside constraints

We consider the model indicated by equation (7), (11) – (17) and we set:

$$b_{p,q,t} = \infty. \tag{22}$$

Equation (22) ensures only airside constraints are active since the decision variables related to passenger demand, $y_{p,q,t}$, are not constrained in any way.

We refer to the model indicated by equation (7), (11) – (17) with $b_{p,q,t} = \infty$ as the A-FGAP model.

ii) Active airside and landside constraints – passenger demand cannot exceed a fixed declared capacity

We consider the model indicated by equation (7), (11) – (17) and we set:

$$b_{p,q,t} = C_{p,q}, \quad t \in K \tag{23}$$

where $C_{p,q}$ is the fixed, declared capacity of facility p in terminal q during a time step t of 5 min.

We assume fixed hourly declared capacity for each facility. We also assume that the number of passengers per hour is distributed uniformly over time.

Equation 23 ensures that for a given flight-to-gate assignment, passenger demand at any facility in the airport is at most the declared capacity of the facilities.

We refer to the model indicated by equation (7), (11) – (17) with $b_{p,q,t} = C_{p,q}$ as the DC-FGAP model.

iii) Active airside and landside constraints – maximum passenger waiting time drives landside constraints

In this section, we first introduce the model for the expected passenger waiting time at airport facilities. Using this, we dynamically adjust the parameter $b_{p,q,t}$ in constraint (17), such that the expected maximum passenger waiting time does not exceed a user-defined threshold $W^T > 0$.

1. Expected maximum waiting time for a passenger at a facility:

We define a peak demand period $n \in U_{p,q}$ for facility p in terminal q as a period where the passenger demand per time step exceeds the average demand per time step, where

$U_{p,q}$ is the set of peak periods at facility $p \in H$ in terminal $q \in T$. The expected maximum waiting time for facility p in terminal q during peak period n, denoted by $W_{p,q,n}$, is estimated (Solak, Clarke, and Johnson 2006, 2009) to be:

$$W_{p,q,n} = \frac{E[L_{p,q,n}] + 1.65\sqrt{Var[L_{p,q,n}]}}{C_{p,q}}, \tag{24}$$

where $C_{p,q}$ is the declared capacity of facility p in terminal q during a time step with a length 5 min, and $L_{p,q,n}$ is the queue length during peak period n at facility p in terminal q.

To approximate $L_{p,q,n}$, we use a parabolic approximation of the passenger demand curve in a discrete time-system (Solak, Clarke, and Johnson 2009). The parabolic approximation of peak demand period n for facility p in terminal q, denoted by $y^{pb}_{p,q,t}$, is modeled as follows:

$$y^{pb}_{p,q,t} = \max_t (y_{p,q,t}) - a_{p,q,n}\left(t - \frac{T_{p,q,n}}{2}\right)^2, \tag{25}$$

with $a_{p,\,q,n} = 4\left(\max_t (y_{p,q,t}) - E[y_{p,q,t}]\right)/T^2_{p,q,n}$ and $T_{p,q,n} = t^e_{p,q,n} - t^s_{p,q,n}$.

2. Dynamically setting the value of $b_{p,q,t}$ in constraint (17) using $W_{p,q,t}$:

We dynamically adjust the parameters $b_{p,q,t}$ in constraint (17) such that the expected maximum waiting time for passengers at the airport facilities considered does not exceed a user-defined threshold W^T. We achieve this as follows:

1) we set $b_{p,q,t} = \infty$ in constraint (17)
2) we solve the model in equation (7), (11) – (17)
3) we determine the expected maximum passenger waiting time $W_{p,q,n}$ associated with the flight-to-gate assignment obtained, for all $p \in H,\ q \in T,\ n \in U_{p,q}$
4) we check if $W_{p,q,n} > W^T$ and if so, the value of $b_{p,q,t}$ is decreased as follows:

$$b_{p,q,t} = \max_{t \in [t^s_{p,q,n} - t^e_{p,q,n}]} (y_{p,q,t}) - \Delta_s,\ t \in [t^s_{p,q,n} - t^e_{p,q,n}], \tag{26}$$

where $t^s_{p,q,n}$ and $t^e_{p,q,n}$ denote the start and end time of peak period n at facility p in terminal q, respectively, and Δ_s is an adjustment parameter. We select a value of $\Delta_s = 1$. This ensures that the optimality of the final solution obtained for the FGAP model in equation (7), (11) – (17) is not compromised by setting a value of Δ_s too large, and

5) We repeat steps ii), iii), iv) until $W_{p,q,n} \leq W^{T\,\prime}$ for all $p \in H,\ q \in T,\ n \in U_{p,q}$.

We refer to this FGAP model where the expected passenger waiting times constraints the landside facilities (see equation (7), (11) – (17)), as the WT-FGAP model.

4. Results

This section presents the results of the robust, landside-airside FGAP models. First, we describe the data used to illustrate our models. Next, we provide the results for the A-FGAP, DC-FGAP and WT-FGAP models, respectively. The A-FGAP model is used as

a baseline since this model considers airside constraints only. The DC-FGAP model ensures that the passenger demand at any facility does not exceed a fixed capacity. The WT-FGAP model dynamically adjusts capacity limits such that the passenger maximum waiting time does not exceed a pre-defined threshold. The results are obtained for one day of operations at Schiphol airport (AMS). For computational reasons, a compression factor of 5 is applied to the flight schedule. All the models are solved using IBM CPLEX Optimization Studio (IBM, 2019) implemented on a computer with a 2.3 GHz Intel Core i5 processor and 16GB of DDR3 RAM.

4.1. Data description

Airport terminal topology and passenger streams

We assume a generic topology of an airport terminal (Figure 10). On the public side, the airport consists of the departure/arrival area. On the non-public side, the airport consists of the lounges/waiting area and the gates. Terminals are connected in the departure/arrival area without passenger movement restrictions. In the lounges/waiting area, terminals are connected with passenger movement restrictions between, in the case of The Netherlands, Schengen and Non-Schengen areas.

We consider three generic passenger streams at the airport: i) departing, ii) arriving and iii) transfer passenger streams. Passengers from arriving flights feed into arriving and transfer passenger streams. Passengers on departing flights are contained in the transfer and departing passenger streams. The stream of arriving passengers moves from the non-public area to the public area in the same terminal. The stream of departing passengers consists of two substreams with passengers that enter the non-public area from the public area in the same terminal and the non-public area from a different terminal. The transfer passenger stream consists of three substreams: an incoming stream, an outgoing inter-terminal transfer passenger stream and an intra-terminal transfer passenger stream. We also assume that all transfer passengers are captured by the intra-terminal transfer passenger substream.

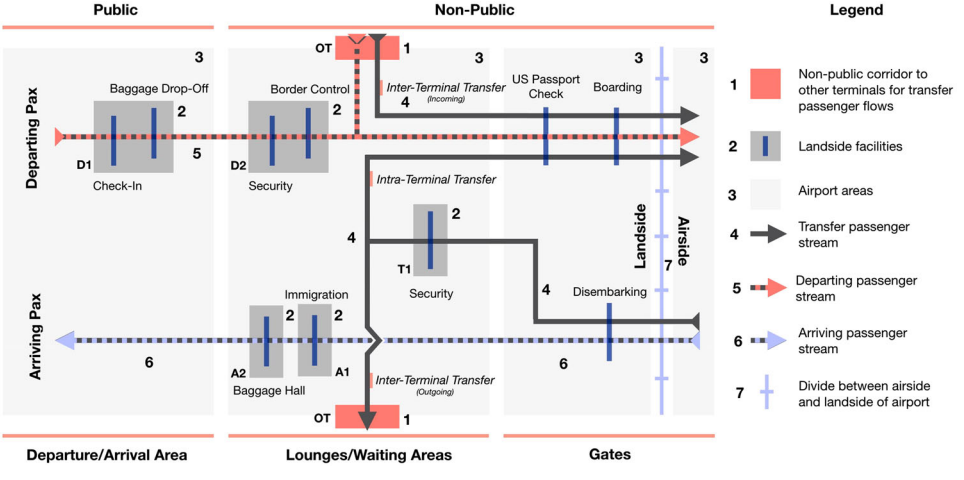

Figure 10. Generic topology of an airport terminal.

Table 1 shows the airport facilities considered in this paper, together with their associated passenger streams, as indicated in Figure 15. For departing passenger streams, the check-in and baggage drop-off facilities (D1) and the security facilities and border control (D2) are considered. For arriving passenger streams, immigration (A1) and the baggage claim area (A2) are considered as distinct facilities. Finally, for transfer passenger streams, security services (T1) are considered.

Table 2 shows the expressions of $t^s_{i,p,q}$ and$t^e_{i,p,q}$ for facilities (A1), (A2), (T1), (D1) and (D2), where $T_1 = 10$ min is the time for arriving and transfer passengers to walk from the gate to facilities (A1) and (T1), respectively, $T_2 = 10$ min is the time for passengers to proceed from facility (A1) to (A2), $T_3 = 45$ min is the time between the first and last passenger disembarking from the aircraft, T_4 is the time between the first and last passenger of flight segment $i \in N_d$ that uses facility (D1), $T_5 = 10$ min is the time for passengers to proceed from facility (D1) to (D2) and T_6 is the time between the last passenger of flight segment $i \in N_d$ to use facility (D1) and the STD of flight segment $i \in N_d$. Lastly, we denote by T_4 the time in minutes between the first and last passenger of a flight that uses check-in facilities and T_6 is the time in minutes between the time the last passenger of a flight uses check-in facilities and the STD of that flight. The values of T_4 and T_6 are derived from the daily flight schedule.

Estimated hourly capacity of facilities in the airport terminal

Table 3 indicates the estimated hourly declared capacity of facilities A1, A2, T1, D1, D2. We note that AMS has four terminals, so we specify the capacity for these facilities for each of terminal. Also, Terminal 1 and Terminal 4 only serve flights with a Schengen

Table 1. Overview of landside facilities.

	Group Name	Pax Stream	Facilities Included
A1	Immigration	Arriving	Passenger immigration services
A2	Baggage Claim	Arriving	Baggage claim
T1	Security	Transfer	Transfer security services
D1	Check-In	Departing	Check-in & baggage drop
D2	Security & Border Control	Departing	Security services & border control

Note: Facility-specific expressions for $t^s_{i,p,q}$ and$t^e_{i,p,q}$ (see Section 2.3) are given in Table 2.

Table 2. Expressions of $t^s_{i,p,q}$ and$t^e_{i,p,q}$ for terminal facilities.

Facility	$t^s_{i,p,q}$	$t^e_{i,p,q}$
A1	$STA_i + T_1$	$STA_i + T_1 + T_3$
A2	$STA_i + T_1 + T_2$	$STA_i + T_1 + T_2 + T_3$
T1	$STA_i + T_1$	$STA_i + T_1 + T_3$
D1	$STD_i - T_4 - T_6$	$STD_i - T_6$
D2	$STD_i - T_4 + T_5 - T_6$	$STD_i + T_5 - T_6$

Table 3. Overview of estimated declared capacity (passengers) per hour of landside facilities at AMS.

Terminal	A1	A2	T1	D1	D2
Terminal 1	N/A	3,420	N/A	1,690	3,040
Terminal 2	2,840	2,840	3,420	1,380	2,700
Terminal 3	2,500	2,500	1,080	1,230	2,220
Terminal 4	N/A	990	N/A	495	900

clearance level. As such, facilities (A1) and (T1) are not present in these terminals and, thus, their capacity is not shown in Table 3.

Flight schedule

We consider the scheduled arrival and departure flight times at AMS on July 4, 2018, with a total of 575 arrival and 549 departure flights. The month of July accounted for 9.53% of the annual number of passengers at AMS in 2018), indicating that this month has a high passenger demand. Each arriving/departing flight has a scheduled arrival/departure time.

4.2. Assignment of flight segments to gates

In this section we show the assignment of flights to gates taking into account: i) only airside constraints (A-FGAP model), ii) both airside and landside constraints with fixed landside facility capacities (DC-FGAP model), and iii) both airside and landside constraints, without fixed facility capacities, and passenger waiting time constraints (WT-FGAP model). For all three models, we consider a user-defined maximum overlap probability of $r = 5\%$.

Figure 11 shows the assignment of flights to gates when considering only airside constraints (the A-FGAP model).

The results show that functional and parking flight segments have a varying length, with a minimum duration of 45 and 90 min, respectively. On average, a buffer time of 109.5 min is allocated between flight segments. The minimum separation time between functional flight segments is 25 min. One functional flight segment is assigned to a platform. All flight splitting options are used, except flight splitting option v) (see Section 2.1).

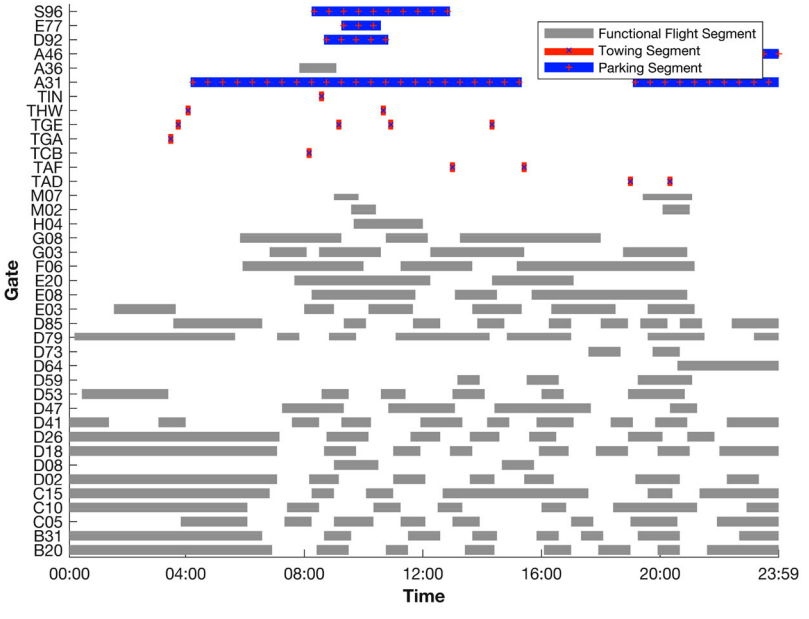

Figure 11. Assignment of flight segments to gates under the A-FGAP model.

Figure 12 shows the assignment of flights to gates when considering both airside and landside constraints with fixed landside facility capacities (the DC-FGAP model). As in the case of the A-FGAP model, the length of the flight segments varies between 45 and 90 min. However, the average buffer time is slightly smaller than in the case of the A-FGAP model, with a mean value of 104.9 min and a standard deviation of 9.5 min. The minimum separation time between functional flight segments is also 25 min. Three functional flight segments are assigned to a platform. All flight splitting options are used, except for flight splitting option v) (see Section 2.1).

Figure 13 shows the assignment of flights to gates when considering both airside and landside constraints without fixed facility capacities, and passenger waiting time constraints (the WT-FGAP model). We note that we ensure that the maximum waiting time for passengers does not exceed a waiting threshold W^T = 25 min. We reached our solution after four iterations (see equation (26)) As for the A-FGAP and the DC-FGAP models, the length of the flight segments varies between 45 and 90 min. Here, the average buffer time is 105.3 min, which is slightly more than in the case of the DC-FGAP model, but less than the A-FGAP model. The standard deviation of the buffer time has a value of 9.3 min and is marginally larger compared to the standard deviation found using the DC-FGAP model. The minimum separation time between functional flight segments is also 25 min. Here, only one functional flight segment is assigned to a platform. All flight splitting options are used, except for flight splitting option v) (see section 2.1).

Figures 14 and 15 indicate the assignment of functional flight segments under the DC-FGAP and WT-FGAP models relative to the A-FGAP model, respectively. For example, Figure 15 shows that 13.7% and 14.5% of all functional flight segments are assigned to concourse C if the DC-FGAP model and the A-FGAP model are

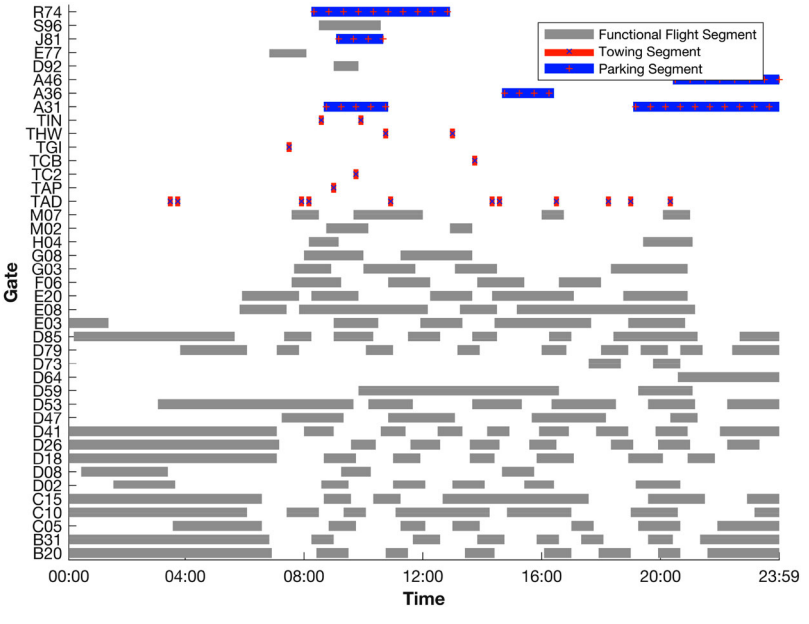

Figure 12. Gate assignment planning obtained using the DC-FGAP model.

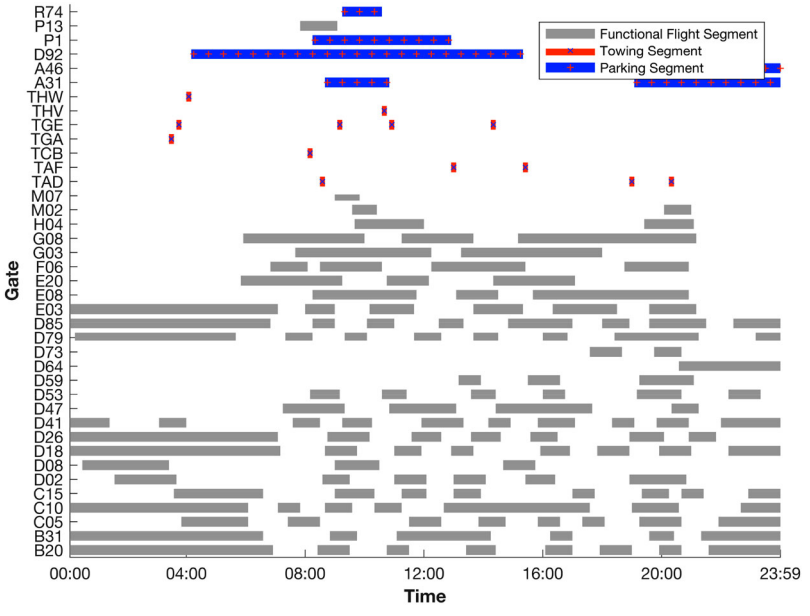

Figure 13. Gate assignment planning obtained using the WT-FGAP, W^T = 25 min.

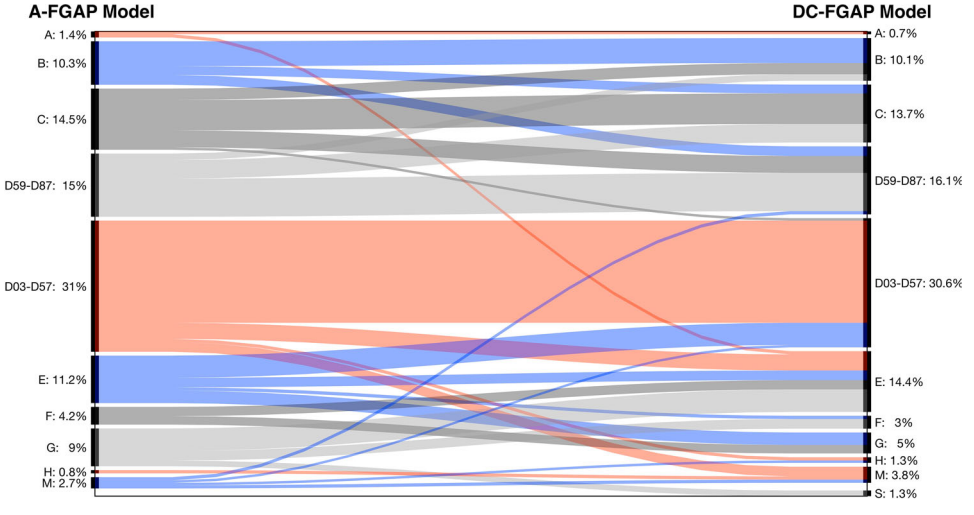

Figure 14. Comparison of functional flight segment allocation to gates: DC-FGAP model vs. A-FGAP model.

used, respectively. Reallocation of functional flight segments between concourses occurs when different FGAP models are used due to the equivalence in characteristics between gates in different concourses. For example, piers in concourses B, C and D59–87 have similar size and customs characteristics. A clear division between concourses that serve Schengen flights (B, C, D59–87, M) and concourses that serve Non-Schengen flights (A, D03-D57, E, F, G, H, S) is observed. The WT-

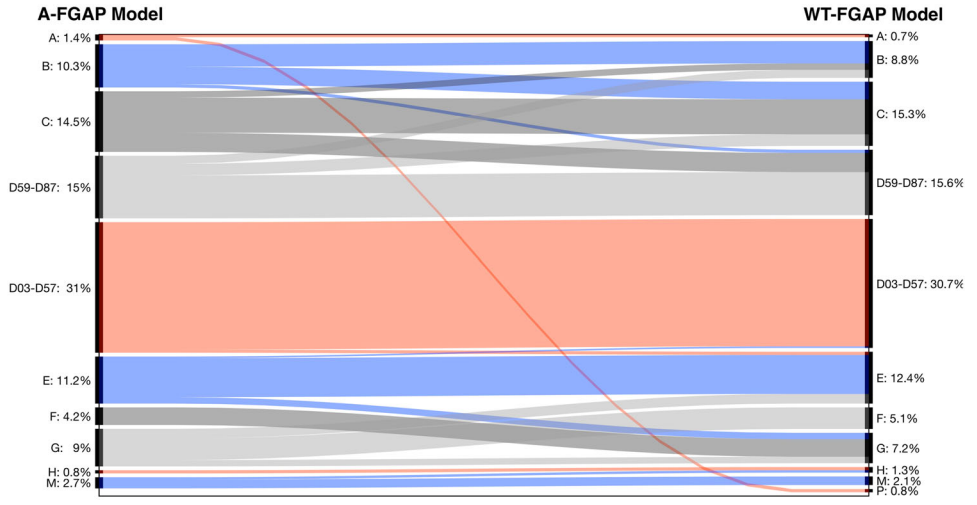

Figure 15. Comparison of functional flight segment allocation to gates: WT-FGAP model vs. A-FGAP model.

FGAP model imposes passenger demand constraints that are less strict compared to the DC-FGAP model. Thus, fewer deviations from the solution of the A-FGAP model are needed when using the WT-FGAP model.

4.3. Landside performance metrics

In this section we analyse the impact of the flight-to-gate assignment on landside facilities by means of two metrics: the demand-capacity ratio and the expected maximum passenger waiting time.

We define the demand-capacity ratio for facility p in terminal q, denoted by $m_{p,q}$, to be the ratio between the maximum passenger demand imposed on facility p in terminal q and the declared capacity $C_{p,q}$, as follows:

$$m_{p,q} = \max_t \frac{y_{p,q,t}}{C_{p,q}} \cdot 100\%, \quad p \in H,\ q \in T \tag{27}$$

We define the maximum expected passenger waiting time over all peak periods n at facility p in terminal q, denoted by $W^{max}_{p,q}$, as follows:

$$W^{max}_{p,q} = \max_n (W_{p,q,n}), \quad p \in H,\ q \in T \tag{28}$$

Figure 16 shows the demand-capacity ratios for all facilities and terminals under the A-FGAP model, which considers airside constraints only since the values of $b_{p,q,t}$ are not bounded. Thus, $m_{p,q}$ can be larger than 100%, e.g. $m_{T1,3} = 250\%$ and all facilities in Terminal 2 and facility (A2) in Terminal 4 have a $m_{p,q} > 100\%$ Facilities (D1) and (D2) feature a value of $m_{p,q} < 30\%$. Figure 17 shows the expected maximum waiting times for all facilities and terminals under the A-FGAP model. For facilities (T1) in Terminal 3 and (D1) in Terminal 2, $W^{max}_{p,q} > W^T$. Due to a short duration of the peak demand periods at facility (T1) in Terminal 2, the value of $m_{p,q} > 100\%$, but $W^{max}_{p,q} < 1$min.

Figure 16. A-FGAP: demand-capacity ratios $m_{p,q}$.

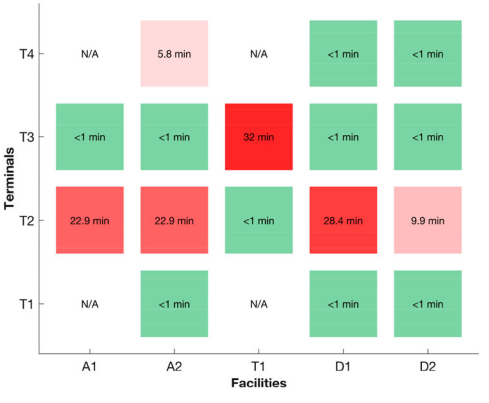

Figure 17. A-FGAP: maximum waiting time $W^{max}_{p,q}$

Figure 18 shows the demand-capacity ratios for all facilities and terminals under the DC-FGAP model, which imposed constraints such that $y_{p,q,t} \leq C_{p,q}$. Thus, $m_{p,q} \leq 100\%$ for all facilities and terminals. Facilities (A1) and (A2) in Terminal 3 and 4 and all facilities in Terminal 2 and 3 have a $m_{p,q}$ equal or close to 100%. As expected, Figure 19 shows that $W^{max}_{p,q} < 1$ min for all facilities and terminals.

Figure 20 shows the demand-capacity ratios for all facilities and terminals at AMS under the WT-FGAP model, which dynamically sets the values of the parameters $b_{p,q,t}$ such that all $W^{max}_{p,q} \leq W^T$. Facility (A2) in Terminal 4, facilities (A1), (A2), (T1) in Terminal 3 and all facilities in Terminal 2 have $m_{p,q} > 100\%$.

Figure 21 shows the expected maximum waiting times for all facilities and terminals at AMS under the WT-FGAP model. For facility (A2) in Terminal 3, facility (T1) in Terminal 3 and facilities (A1), (A2) and (D1) in Terminal 2, $W^{max}_{p,q} > 5$ min. All values of $W^{max}_{p,q} < W^T$, as imposed by the WT-FGAP model. By construction, all values of $m_{p,q}$ of the WT-FGAP model are bounded; the lower and upper bounds are the values of

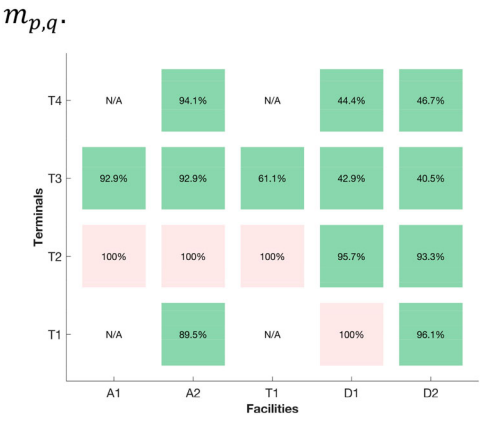

Figure 18. DC-FGAP: demand-capacity ratios $m_{p,q}$.

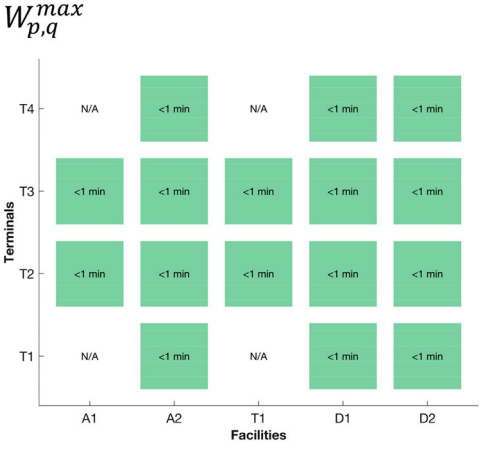

Figure 19. DC-FGAP: maximum waiting time $W_{p,q}^{max}$.

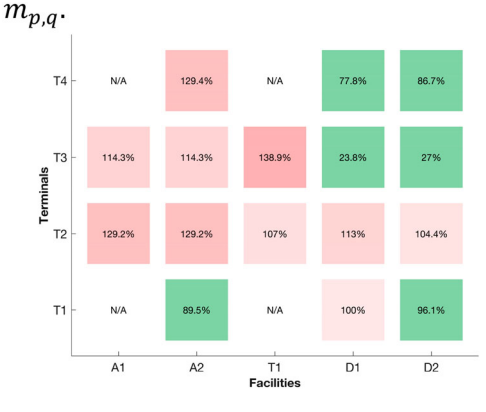

Figure 20. WT-FGAP: demand-capacity ratio $m_{p,q}$.

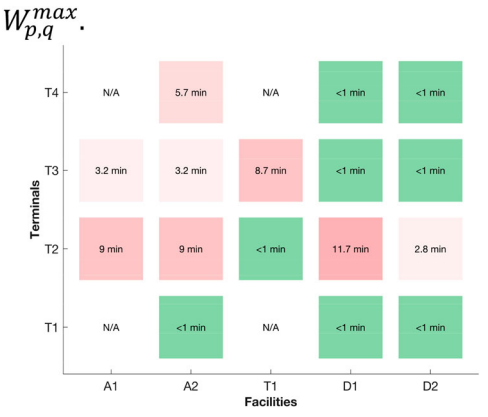

Figure 21. WT-FGAP: maximum waiting time $W_{p,q}^{max}$.

$m_{p,q}$ of the DC-FGAP model and A-FGAP model, respectively. The same bounds exist for $W_{p,q}^{max}$.

5. Conclusions

In this paper we have developed robust flight-to-gate assignment models that have considered both airside and landside constraints. For the landside, we considered three strategies: i) no constraints for passenger capacity, ii) a fixed declared capacity for each landside facility, acts as a threshold for the maximum number of passengers to use a facility in a period of time; and iii) a threshold on the maximum waiting time that passengers experience at landside facilities. We determined optimal flight to gate assignments under the three types of landside constraints and provided estimates for the waiting times for passengers inside the airport. We have also shown how the different types of landside constraints drive changes in the assignments of flights to gates. To illustrate our models, we considered one day of operations at Amsterdam Schiphol Airport. Overall, our model supports the design of a robust, integrated airside-landside assignment of flights to gates at an airport.

Future work includes the development of improved flight presence probabilities and implementation of flight-specific input. We also plan to improve the compression factor for the flight schedule using decomposition methods.

Disclosure statement

No potential conflict of interest was reported by the author(s).

ORCID

J. L'Ortye http://orcid.org/0000-0002-1106-2552

References

Bolat, A. 2000. "Procedures for Providing Robust Gate Assignments for Arriving Aircraft." *European Journal of Operational Research* 120 (1): 63–80.

Bouras, A., M. A. Ghaleb, U. S. Suryaatmaja, and A. M. Salem. 2014. "The Airport Gate Assignment Problem: A Survey." *The Scientific World Journal* 923859. doi:10.1155, 2014.

Castaing, J., I. Mukherjee, A. Cohn, L. Hurwitz, A. Nguyen, and J. J. Müller. 2016. "Reducing Airport Gate Blockage in Passenger Aviation: Models and Analysis." *Computers & Operations Research* 65: 189–199.

Chun, H., and R. Mak. 1999. "Intelligent Resource Simulation for an Airport Check-in Counter Allocation System." *Transactions on Systems, Man and Cybernetics-Part: Applications and Reviews* 29 (3): 325–335.

Diepen, G., J. Van Den Akker, J. A. Hoogeveen, and J. Smeltink. 2012. "Finding a Robust Assignment of Flights to Gates at Amsterdam Airport Schiphol." *Journal of Scheduling* 15 (6): 703–715.

IBM. 2019. *IBM cplex optimization studio*, April 2019. URL https://www.ibm.com/analytics/cplex-optimizer.

Kim, S. H., E. Feron, J.-P. Clarke, A. Marzuoli, and D. Delahaye. 2017. "Airport Gate Scheduling for Passengers, Aircraft, and Operations." *Journal of Air Transportation* 25 (4): 109–114.

Kusumaningtyas, I., and G. Lodewijks. 2013. "On the Application of Accelerating Moving Walkways to Support Passenger Processes in Amsterdam Airport Schiphol." *Transportation Planning and Technology* 36 (7): 617–635.

Li, Y., X. Gao, Z. Xu, and Z. Zhou. 2018. "Network-based Queuing Model for Simulating Passenger Throughput at an Airport Security Checkpoint." *Journal of Transport Management* 66: 13–24.

Manataki, I., and K. Zografos. 2009. "A Generic Systems Dynamics Based Tool for Airport Terminal Performance Analysis." *Transportation Research Part C* 17: 428–443.

Mangoubi, R., and D. F. Mathaisel. 1985. "Optimizing Gate Assignments at Airport Terminals." *Transportation Science* 19 (2): 173–188.

Schaijk, O., and H. Visser. 2017. "Robust Flight-to-Gate Assignment Using Flight Presence Probabilities." *Transportation Planning and Technology* 40 (8): 928–945.

Seker, M., and N. Noyan. 2012. "Stochastic Optimization Models for the Airport Gate Assignment Problem." *Transport Research Part E: Logistics and Transportation Research* 48 (2): 438–559.

Solak, S., J. Clarke, and E. Johnson. 2006. "Airport Terminal Capacity Planning Using Delay Time Approximations and Multistage Stochastic Programming." *Georgia Institute of Technology*. https://citeseerx.ist.psu.edu/viewdoc/download?doi=10.1.1.61.7254&rep=rep1&type=pdf.

Solak, S., J.-P. B. Clarke, and E. L. Johnson. 2009. "Airport Terminal Capacity Planning." *Transportation Research Part B: Methodological* 43 (6): 659–676.

van Dijk, N., and E. van der Sluis. 2006. "Check-in Computation and Optimization by Simulation and ip in Combination." *European Journal of Operational Research* 171: 1152–1168.

Yan, S., and C. Chang. 1997. "A Network Model for Gate Assignment." *Journal of Advanced Transportation* 32 (2): 176–189.

Yan, S., and C. Huo. 2001. "Optimization of Multiple Objective Gate Assignments." *Transport Research Part A: Policy and Practice* 35: 413–432.

Yu, C., D. Zhang, and H. Lau. 2016. "Mip-based Heuristics for Solving Robust Gate Assignment Problems." *Computers and Industrial Engineering* 93: 171–191.

Yu, C., D. Zhang, and H. Lau. 2017. "An Adaptive Large Neighborhood Search Heuristic for Solving a Robust Gate Assignment Problem." *Expert Systems with Applications* 84: 143–154.